Studies on the Surface Structure of Porous Materials

By Akie TSURUIZUMI

(Received December 29, 1960)

It has been generally accepted that the adsorption of gases on adsorbents such as active carbon and silica gel is both physical and chemical in nature, the latter being caused by the formation of complex surface compounds with residual active groups as well as by an ion exchange effect on the surface. The chemisorption plays a role in the earlier stage of the adsorption process, while the general behavior of the adsorption is characterized by the physical behavior.

Pore structure of the surface, which is important for both the theoretical and practical studies, could be visualized by combining

various methods such as porosimetries and adsorption measurements. A preferential physical adsorption of adsorbates with various molecular sizes could be used most effectively for classification of the pore-sizes.

In the present paper, the pore structures of various adsorbents such as active carbon and silica gel were studied. The results of adsorption measurements with water vapor and various organic vapors, the BET method using nitrogen, and mercury and water prosimetry were analyzed, and the size, shape and chemical nature of the pores were discussed in detail.

An emphasis was placed on the deviations from the prevailing theories, which are based on a simple pore model such as the cylindrical one. The analysis of the deviations enabled us to depict the shape of the pore, being of narrow-neck or ink-bottle shape. In addition, a new term, 'sieving coefficient' was proposed, which would be quite profitable for classification of the adsorbents.

Theoretical

The pores are classified into the following three groups: micro-pores, ca. 10Å in radii; transitional pores, 100~500Å; micro-pores, 10000Å. The transitional and micro-pore distributions are determined empirically by a mercury porosimetry[1]. The micro-pore distribution is calculated by Thomson's formula,

$$r=-\frac{2v\sigma\cos\theta}{RT\ln P/P_0} \tag{1}$$

where v is the molecular volume, θ the contact angle, σ the surface tension, r the pore radius, P the vapor pressure of the meniscus, and P_0 that of the bulk phase.

A total volume of pores with a radius in a range between r and $r+dr$ is represented by

$$dv=D(r)dr \tag{2}$$

where v is the total volume of the pores, and $D(r)$ the distribution function of the pore radii. The function $D(r)$ is obtained by graphical differentiation of a curve drawn by plotting the total amount of adsorption against the radii of the pores. A plot of $dv/d\log r$ vs. $\log r$ was similar to the Gaussian probability curve.

Thomson's equation is implicitly based on the following assumptions: i) Adsorption of water is caused by the capillary condensation. ii) The pore is cylindrical in shape with a uniform diameter. iii) The water adsorbed in the pore has the same density as that in bulk phase.

Cohan[2], McBain[3] and Higuchi[4] have pointed out that the size distribution function of pores having diameters less than 10Å can not be calculated by Thomson's equation. If the radii of pores are less than 10Å, the condensation of water vapor inside the pore is impossible, because the diameter of the void space in the pore is reduced to 2~3 molecular sizes by preliminary formation of a monolyer on the inside wall in the earlier stage of the adsorption process.

In the range of higher radius, a minor correction for pore radius less than six per cent is necessary[5]. This is due to the reduction of the pore space by the formation of the adsorption film on the wall. This correction was, however, not applied in the present study. Actually, pore-size distribution curves obtained by using Thomson's equation are in good agreement with those obtained from the adsorption of nitrogen as has been shown by Joyer[6], with those obtained by the adsorption of benzene vapor and by the mercury porosimetry reported by the present author[7].

The radius of a cylindrical pore is given by the equation[8]

$$pr=2\pi\sigma\cos\theta \tag{3}$$

where p is the applied pressure to press the mercury into the pore, σ the surface tension of mercury, r the redius of the pore and θ the contact angle.

Expressing p in kg./cm^2, r in cm., and putting $\delta=480$ dyn./cm. and $\theta=140°$C[9,10], Eq. 3 is reduced to

$$pr=7.5\times10^{-4} \tag{4}$$

If the pores are ink-bottle or bottle-neck shaped, the appearent radii obtained by the porosimetry are those of narrow-neck shape, being less than the true ones.

Experimental

Materials.—*Sugar Charcoals* (S_3, S_4, SZ_3, SZ_4).—S_3, S_4[11]: An aqueous solution of commercial white sugar decolored with an active carbon was passed through a column of ion exchange resins (Amberlite

1) H. L. Ritter and L. C. Drack, *Ind. Eng. Chem., Anal. Ed.*, **17**, 782 (1945).

2) L. H. Cohan, *J. Am. Chem. Soc.*, **60**, 433 (1938).

3) J. W. McBain, ibid., **57**, 691 (1935).

4) I. Higuchi, *Sci. Pap. Inst. Phys. Chem. Res.*, **20**, 130 (1941).

5) M. M. Dubinin, *Quart. Rev.*, **9**, 109 (1955).

6) L. G. Joyer, E. P. Barset and R. Skold, *J. Am. Chem. Soc.*, **73**, 3155 (1951).

7) A. Tsuruizumi, *J. Chem. Soc. Japan, Pure Chem. Sec. (Nippon Kagaku Zasshi)*, **81**, 870 (1960).

8) E. W. Washburn, *Proc. Natl. Acad. Sci.*, **7**, 115 (1921).

9) H. L. Ritter and L. C. Drake, *Ind. Eng. Chem., Anal. Ed.*, **17**, 782, 787 (1945).

10) A. J. Juhola and E. O. Wiig, *J. Am. Chem. Soc.*, **71**, 2069, 2078 (1949).

11) A. Tsuruizumi, *J. Chem. Soc. Japan, Pure Chem. Sec. (Nipoon Kagaku Zasshi)*, **79**, 266 (1957).

TABLE I. CLASSIFICATION OF PORE VOLUME

Sample	A v_1 Micro-P. vol. to 50 Å (r) cc./g.	B[a] v_2 Trans.-P. vol. 75~1000 Å cc./g.	C[b] v_3 Macro-P. vol. 1000~43000 Å cc./g.	D Pressed total mercury vol. B+C cc./g.	E V_t Total pore vol. A+D=A+B+C cc./g.
S_3	0.1205	0.0152	0.0590	0.0742	0.1947
S_4	0.1554	0.0162	0.0410	0.0572	0.2126
SZ_3	0.7950	0.0350	0.0680	0.1030	0.8980
SZ_4	0.8850	0.0370	0.2200	0.2570	1.1420
M. S.[c]	0.2140	0.0680	0.1330	0.2010	0.4150
Silica[d]	0.3750	0.0800	0.0410	0.1210	0.4960

a) B, b) C calculated from mercury porosimetry.
c) Molecular sieve 5 A.
d) Silica gel No. 28.

IRA 400 and IRC 120) repeatedly until its electrical conductivity was reduced to as low as 4~6 $\mu\mho$/cm. The crystals of the sugar purified by recrystallization from ethanol were dried at 40°C under 5~10 mmHg. The ashes in 10 g. of the purified sugar were undetectable with a chemical balance. The sugar placed on a quartz boat in a quartz combustion tube in an electric furnace was carbonized in a stream of nitrogen gas with a flow rate of 20~30 ml./min. The traces of oxygen in this were removed beforehand by passing through a layer of heated reduced copper. The temperature of the furnace was raised at a rate of 5°C/min., and then kept at a required temperature for 30 min. The rate of temperature rise was a factor to determine the pore structure. Carbonization temperatures and yields were as follows: S_3, 800°C and 23.44%; S_4, 1000°C and 21.30%. Granules of 70~100 meshes were collected with sieves. Spectroscopic analysis: Al (−), Si (+),·····.

SZ_3, SZ_4: A mixture of 10 g. of the purified sugar and 20 g. of zinc chloride (G. P. grade) with a few drops of hydrochloric acid was heated to 200°C on a evaporating dish. The charcoals obtained by the same carbonization process as that mentioned above from the residues were boiled with hydrochloric acid (1 : 1) to remove zinc chloride, washed with distilled water till pH values of the filtrates became 5~6, and dried for 4~6 hr. at 150~170°C. Granules of 70~100 meshes were collected. Ashes in 1 g. of the sample were undetectable with a chemical balance. No traces of zinc were detected by the dichizon method[12]. Spectroscopic analysis: Al (−), Mg(±), Si(+).

*Molecular Sieve 5A**. — Composition: $Me^{12}/n\{(AlO_2)_{12}-(SiO_2)_{12}\}27-30H_2O$, (Me: Ca, Na). Highly polar. Pore diameter noted by the manufacturer was 5 Å.

Silica Gel No. 28. — A gel precipitated from 3 N sodium silicate and 4 N sulfuric acid at a controlled pH of 5.5 was washed with water, electrodialized for 100 hr., dried at 20~30°C, and finally at 120~150°C. 70~100 meshes.

3SZ$_4$, 6SZ$_4$.—A sample of SZ_4 impregnated with 2 per cent nitrobenzene solution of polyvinyl chloride (Geon 103EP) was carbonized by the same method as that mentioned above at 1000°C. The process was repeated three times for $3SZ_4$ and six times for $6SZ_4$. The pore volumes and internal total wall areas were shown in Tables I and II.

TABLE II. TOTAL PORE VOLUME BY WATER OR MERCURY DISPLACEMENT METHODS

Sample	F Water displ. vol. cc./g.	G Mercury displ. vol. cc./g.	H Total pore vol. G−F cc./g.
SZ_3	0.540	1.541	1.001
SZ_4	0.528	1.580	1.051

TABLE III. EQUIVALENT INTERNAL WALL AREA OF EACH OF DISPERSE PORTIONS

Sample	Surface area by $S=2V_t/\bar{r}$: S_1 Surface area of micro-P. $m^2/g.$	S_2 Surface area of trans.-P. $m^2/g.$	S_3 Surface area of macro-P. $m^2/g.$	Surface area BET $m^2/g.$
S_3	241 [8.0][e] (10)[f]	2.4 (125.9)	0.11 (10.000)	400
S_4	380 [7.5] (8.2)	2.5 (125.9)	0.08 (10.000)	450
SZ_3	800 [15] (18.0)	2.0	0.14	1400
SZ_4	1180 [10] (15.0)	6.0	0.44	1600
M. S.[c]	660 [2.0] (6.5)	13.0	2.0	460
Silica[d]	681 [7.5] (11.0)	16.0	0.08	720

e) [Å] maximum distribution radius.
f) (Å) mean radius.

Formic Acid. — A guaranteed grade reagent was dehydrated with a boric acid of high melting point by being allowed to stand for a few days, and distilled under reduced pressure. The process was repeated. N_D^{20}: 1.3716.

n-Propionic Acid and n-Butyric Acid.—Guaranteed grade reagents supplied by Tokyo Oka Co., were

12) E. B. Sandell, "Colorimetric Determination of Metals", Interscience Publishers, Inc., New York (1950).
* The product of Linde Air Product Co., U. S. A.

used without further purification. N_D^{20}: 1.3873 and 1.3990.

n-Valeric Acid.—A guaranteed grade reagent supplied by Tokyo Oka Co., was used without further purification.

Benzene. — A guaranteed grade reagent supplied from Wako Junyaku Co., was dehydrated with metallic sodium and distilled under reduced pressure.

Measurements of Adsorption. — The adsorption of water vapor was measured at 30°C with a quartz spring balance of sensitivity of 2.4630 mg./mm. using a cathetometer graduated to 1/20 mm. The samples were out-gased at various temperatures for 6 hr. under 10^{-5} mmHg. The temperatures are: for sugar carbons, 300~350; for molecular sieve 5A, 250~300; for silica gel No. 28, 150~200°C. The poresize distribution was calculated from the desorption isotherm, the contact angle being assumed to be $\cos\theta = 0.49$[10]. Adsorptions of monocarboxylic acids and benzene were measured with a quartz spring balance at 38±0.1°C. The adsorbents were out-gased by heating at 300~350°C and 10^{-5} mmHg.

Measurement of Pore Volume. — The total pore volume was measured by a water and mercury displacement method using a modified Juhola and Wiig's apparatus[10] shown in Fig. 1. The liquid water was introduced into a flask from an upper reservoir after the samples in the flask adsorbed such an amount of water vapor from a side tube that the adsorption equilibrium was reached. The total pore volume was calculated from the difference of volum of water and mercury displaced.

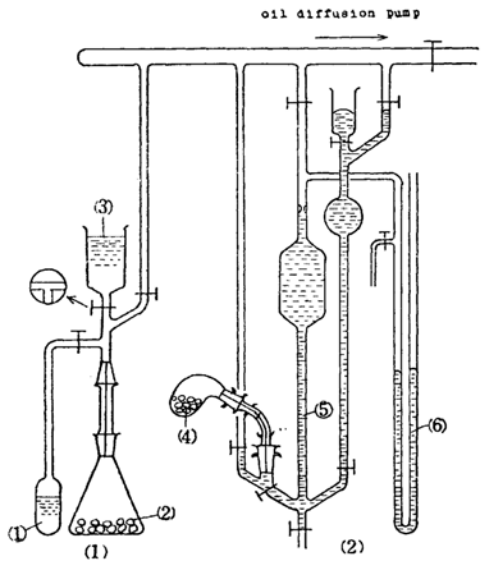

Fig. 1. Displacement volume measurement apparatus.
(1) Apparent density measurement by liquid displacement
(2) Apparent density measurement by mercury displacement
①③ Water ②④ Adsorbent
⑤ Mercury burette
⑥ Mercury manometer

Measurement of BET Area. — The BET surface area was obtained with a usual adsorption apparatus using nitrogen gas as an adsorbate.

Mercury Porosimetry.—A usual mercury porosimeter was used. In order to obtain high accuracy, the diameter of both platinum wire and dilatometer were made as small as possible. The applied pressure was measured with a gauge, and the maximum pressure reached was 1500 kg./cm². The temperature was kept at 0°C.

Experimental Results and Discussion

Pore Distribution.—*S_3 and S_4.*— Plots of $dv/d\log r$ vs. $\log r$ (Å) for the samples S_3 and S_4 are shown in Fig. 2, where a tri-disperse distribution is observed. The peaks are designated as micro-, transitional and macro-pore from left to right in the figure. The shape of the transitional distribution curve is changed by modification of the carbonization or activation condition as is shown later. The distribution curves for a range 3~4 in $\log r$ are not shown as they are less than 10^{-4}, being scaled out.

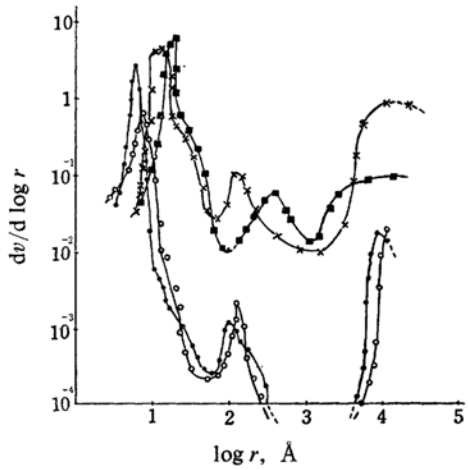

Fig. 2. Pore-size distribution in sugar carbons.
—●— S_4 —■— SZ_3
—○— S_3 —×— SZ_4

SZ_3 and SZ_4. — The pore-size distribution curves are also tri-disperse as a shown in Fig. 2. As is seen in Table IV, the total pore volume estimated from the results of mercury and water displacement method is in good agreement with that calculated as the total sum of the respective volumes of micro-, transitional, and macro-pores. The greater part of the surface areas of the sugar carbons (S_3, S_4, SZ_3 and SZ_4) being composed of the areas of the internal wall of the micro-pores, the number of transitional and macro-pores are too low to give any influence on the adsorption characteristics.

TABLE IV. CLASSIFICATION OF PORE VOLUME

Sample	A v_1 Micro-P. vol. to 50 Å (r) cc./g.	B[b] v_2 Trans.-P. vol. 75~1000 Å cc./g.	C[b] v_3 Macro-P. vol. 1000~43000 Å cc./g.	D Total mercury vol. pressed in B+C cc./g.	E V_t Total P. vol. A+D =A+B+C cc./g.	F[a] Water displ. vol. cc./g.	G[a] Mercury displ. vol. cc./g.	H Total pore vol. G−F cc./g.
SZ_4	0.885	0.037	0.220	0.257	1.142	0.528	1.580	1.051
$3SZ_4$	0.730	0.023	0.079	0.102	0.832	0.539	1.337	0.798
$6SZ_4$	0.620	0.018	0.065	0.083	0.703	0.535	1.207	0.672
S_4	0.155	0.016	0.041	0.057	0.212	—	—	—
Silica gel No. 28	0.375	0.080	0.041	0.121	0.496	—	—	—

a) Pore volume by water and mercury displacement methods.
b) Calculated from mercury porosimetry.

Molecular Sieve 5A. — The micro-pore distribution curves of molecular sieve 5A were obtained by assuming $\cos\theta=1$ in Thomson's equation because of its high polarity. A di-disperse distribution curve with sharp peaks is seen in Fig. 3.

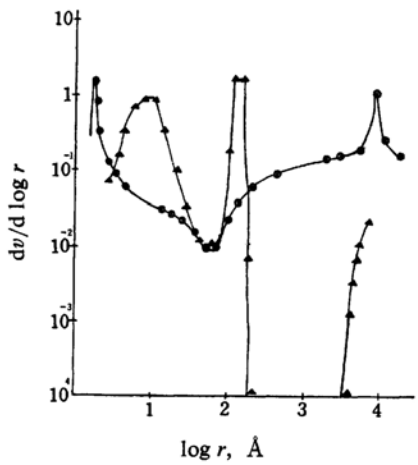

Fig. 3. Pore-size distribution in a silica gel and the molecular sievs 5A.
—▲— SiO_2 gel —⊗— M. S. (5A)

Silica Gel No. 28. — As is seen in Fig. 3, a tri-distribution curve is observed. The curve is, however, broken at a range $\log r=2\sim3$. The macro-pores are presumed to be produced by the secondary treatment, and the distribution curve is originally di-disperse. The total volumes of pores calculated from the respective peaks in the figures are shown in Table IV.

If it is assumed that the pore is a cylinder with a circular section, the total volume of the pores, V_t, and the inner surface area, S, in each peak can be calculated by the formula

$$V_t=\pi(\bar{r})^2L \qquad (5)$$

where $\bar{r}$ is an average radius of pores and L the length of the cylinder. The inner surface area is related to the pore radius by the equation

$$S=2\pi\bar{r}L \qquad (6)$$

In Tables III and V, the inner wall areas calculated by the equation

$$S=2V_t/\bar{r} \qquad (7)$$

and the BET area are compared, where the coincidence is noted only in the case of the silica gel. The discrepancy seen in the tables may be ascribed to both the complexity of the pore structure and a per-sorption[13]. Another minor factor to be taken into account is the difference of densities of nitrogen in the submicro-pore and in bulk phase. The BET area is usually greater than the true area.

TABLE V. INTERNAL WALL AREA OF DISPERSE

Sample	Surface area by $S=2V_t/\bar{r}$: Surface area of micro-P. $m^2/g.$	Surface area of trans.-P. $m^2/g.$	Surface area of macro-P. $m^2/g.$	Surface area by BET $m^2/g.$
SZ_4	1180 [10][a] (15.0)[b]	6.0	0.44	1600
$3SZ_4$	1000 [9.5] (14.5)	3.2	0.16	1460
$6SZ_4$	858 [9.0] (14.1)	2.8	0.13	1300
S_4	380 [7.5] (8.2)	2.5	0.08	450
Silica gel No. 28	681 [7.5] (11.0)	16.0	0.08	720

a) [Å] maximum distribution radius.
b) (Å) mean radius.

The total wall area of the silica gel No. 28, S (total sum of the areas of the micro-pores, transitional pores and macro-pores) is approximately 700 m./g. (Table V), and is in

13) A. Tsuruizumi, *J. Chem. Soc. Japan, Pure Chem. Sec.* (*Nippon Kagaku Zasshi*), **79**, 142 (1957),

agreement with the nitrogen BET area of 720 m./g. The areas obtained by the various fatty acids are ranged between 680 and 750 m^2/g. as will be shown later. These facts prove that there are only a few pores of a narrow-neck or ink-bottle type, which complicate the nature of the adsorption. The radius of the maximum distribution in the molecular sieve 5A is ca. 2Å.

Adsorption of Organic Vapors

The adsorption isotherms of both monocarboxylic acids and benzene vapor were S-shape for all the adsorbents studied, and fit the BET equation well. The adsorption isotherms of benzene vapor on the samples $3SZ_4$ and $6SZ_4$ are shown in Fig. 4. The samples

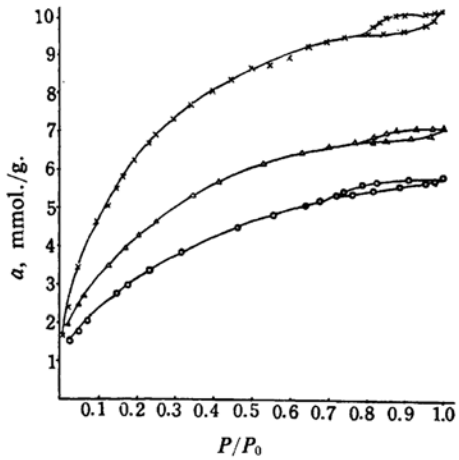

Fig. 4. Adsorption isotherm of benzene.
—×— SZ_4 —△— $3SZ_4$ —○— $6SZ_4$

$3SZ_4$ and $6SZ_4$ were prepared by carbonizing the sample SZ_4 impregnated with the nitrobenzene solution of polyvinyl chloride. The pores of the SZ_4 carbon were filled up to some extent, and the transitional pores were affected most sensitively. The transitional pore distribution curves for SZ_4, $3SZ_4$ and $6SZ_4$ obtained from the desorption isotherms of benzene vapor by using Thomson's equation are shown in Fig. 5, and the full distribution curves drawn by annexing the distribution curves estimated from the data of mercury porosimetry are shown in Fig. 6. The tri-disperse distribution is seen in the figure, and in each peak shift regularly according to the decrease in the pore volumes. The displacement of the transitional peaks are most conspicuous.

The distribution curve of the transitional pores estimated from the benzene adsorption shown in Fig. 4 was slightly higher than those obtained by the mercury porosimetry (Fig. 5).

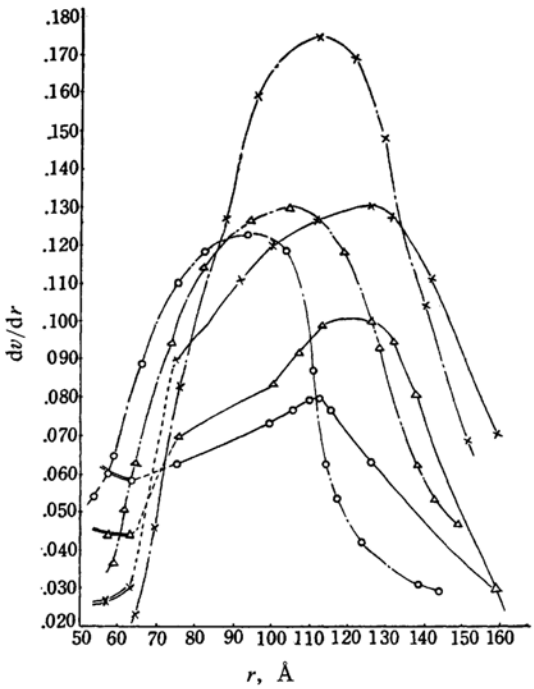

Fig. 5. Distribution of transitional-pores.
—·—· Calculated from benzene adsorption
——— Calculated from mercury porosimetry
═══ Calculated from water vapor adsorption (in the range of micro-pore distribution).
—×— SZ_4 —△— $3SZ_4$ —○— $6SZ_4$

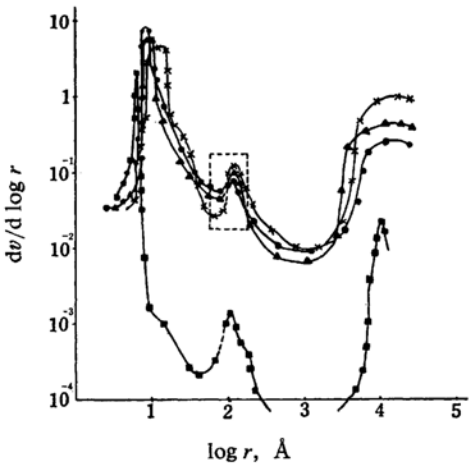

Fig. 6. Carbons pore-size distribution in sugar.
—×— SZ_4 —●— $6SZ_4$
—▲— $3SZ_4$ —■— S_4

The disagreement of the two curves may be ascribed to the errors arising from the application of Thomson's equation which is based on a number of assumptions inadequate in the

present case. Since in the mercury porosimetry no ambiguous assumptions are adduced other than the independency of the contact angle with respect to the applied pressure, the result of the porosimetry is most reliable.

A range of the distribution curve (shown by dotted lines in Figs. 5 and 6) between the micro-pore and transitional pore can not be determined precisely by the mercury porosimetry. Since the curves shown by broken lines with dots in Fig. 5 obtained by the adsorption method using benzene vapor were continuous in full range, it is quite resonable to bridge the gap between the solid line of the mercury porosimetry and the double line of the water adsorption with the dotted line as is shown in Fig. 5.

In the previous papers[11,13,14], the present author has suggested that the pore distribution of the active carbon is tri-disperse. The existence of the micro-pores of about molecular diameter size, the transitional pores (ca. 100Å), and the macro-pores (ca. 100 μ) as cracks or cavities is hereby confirmed.

Effective areas of the adsorbents, calculated from the amounts of adsorbates in a monolayer coverage (Figs. 7, 8 and 9) by using the B-point method[15] are shown in Table VI. The

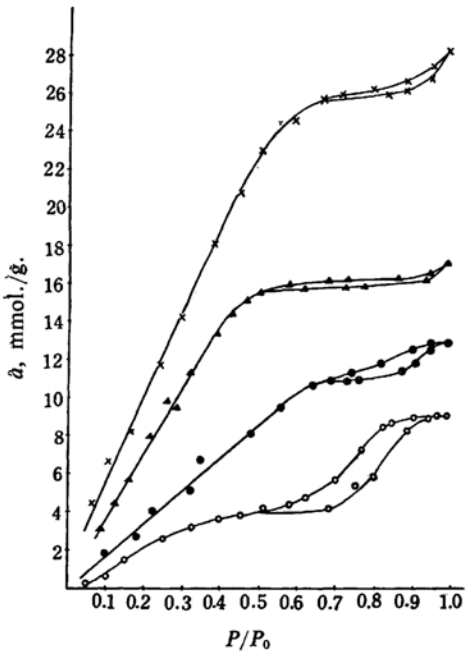

Fig. 7. Adsorption isotherms of *n*-carboxylic acid vapors (SZ_4, 38±0.1°C).
—○— *n*-Butyric acid —▲— Acetic acid
—○— *n*-Propionic acid —×— Formic acid

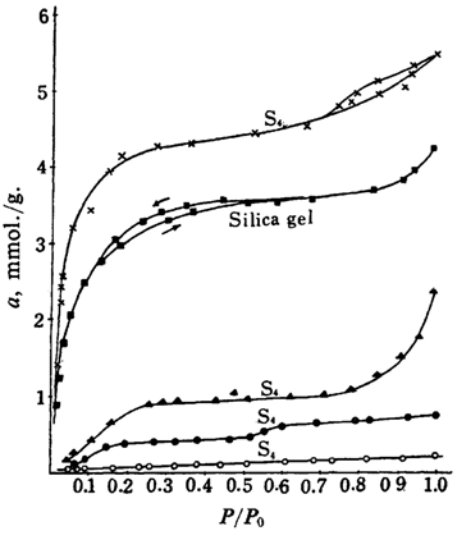

Fig. 8. Adsorption isotherms fo *n*-carboxylic acid vapors (38±0.1°C).
—○— *n*-Butyric acid —×— Formic acid
—●— *n*-Propionic acid —■— Benzene
—▲— Acetic acid

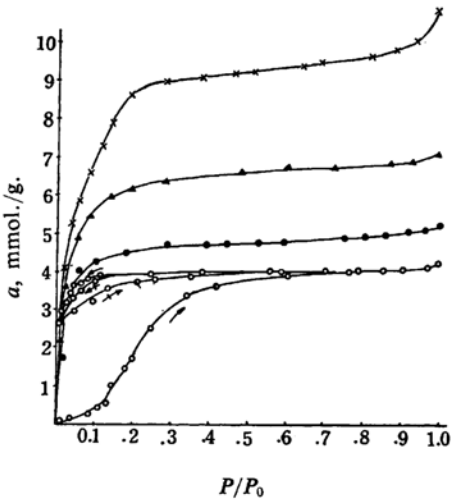

Fig. 9. Adsorption isotherms of *n*-carboxylic acid vapors (silica gel, 38±0.1°C).
⟶ —|→ Adsorption ⟵ ⟶ First process
⟵ ←|— Desorption —|→ ←|— Second process
—○— *n*-Butyric acid —▲— Acetic acid
—●— *n*-Propionic acid —×— Formic acid

sectional areas of the adsorbate molecules used for the calculation of the surface area are listed in Table VI. These were determined by the adsorption on SZ_4, S_4 and silica gel No. 28. The surface areas of sugar carbons obtained with formic and acetic acid are higher than the BET areas, while the higher acids gave lower

14) A. Tsuruizumi, ibid., 79, 273 (1957).
15) A. Blackburn and J. J. Kipling, *J. Chem. Soc.*, 1955, 1493.

TABLE VI. SURFACE AREA OBTAINED FROM ADSORPTION ISOTHERM

Adsorbates	Adsorptive sectional area, Å²	Surface area, m²/g. S_4 [450][a]	SZ_4 [1600]	Silica gel No. 28 [720]
Formic acid	13.38	342.0	2365.0	717.0
Acetic acid	19.58	106.0	1828.0	755.0
n-Propionic acid	25.01	55.0	1600.0	716.0
Benzene	29.13	26.5	1100.0	723.0
n-Heptane	(29.20)[b]	19.0	850.0	680.0
n-Butyric acid	31.35	0.9	717.0	730.0

a) [ ] Surface area from BET method.
b) If adsorptive section is circle from Fig. 10, its radius get 3.05Å as adsorptive sectional area is calculated 29.20Å².

values. This discrepancy can be explained as follows. The molecules of formic and acetic acid are small enough to diffuse into fine pores, and before the formation of a uniform monolayer, a capillary condensation takes place. This increases the apparent surface area. The critical temperatures of the formic and acetic acid are lower than those of the higher acids, but this is not the predominant factor for the earlier occurrence of the capillary condensation. The same situation was found in the adsorption of nitrogen gas as has been reported previously by the present author[13]. These effects of molecular size of the adsorbates on the adsorption characteristics suggest the existence of a number of pores of irregular shapes such as narrow-neck or ink-bottle on the sugar carbon surface.

BET type adsorption isotherms were observed for all the acids on S_4 as is shown in Fig. 8. A surface area of S_4 calculated by the B-point method is, however, remarkably smaller than the nitrogen BET area as is seen in Table VI, and this disagreement increased with the c-number of the acid molecule. This sieving effect of the carbon S_4 is presumed to be due to the special pore-distribution, a greater part of the surface being composed of the micropores of average radius less than 8.2Å. An adsorption isotherm of benzene (non-polar adsorbate) on silica gel No. 28 (polar adsorbent) obtained under the same conditions shows no hysteresis as is shown in Fig. 8, and a surface area calculated by the B-point method was identical with the nitrogen BET area as is shown in Table VI.

As is seen in the Fig. 8, the desorption curve of benzene vapor from the silica gel returns back to the original point, These facts indicate that no chemisorption takes place on the silica gel. BET type adsorption isotherms were observed for various carboxylic acids on silica gel No. 28 as is shown in Fig. 9. Values of the effective surface area of silica gel obtained by the B-point method for the series of carboxylic acids are equal to the nitrogen BET area as is seen in Table VI. These results lead us to conclude that there exist no pores of narrow-neck or ink-bottle shape on the surface of the silica gel, and the pore size is large enough to accommodate such large adsorbate molecules as the carboxylic acids.

In Fig. 9, the anomalous behavior of the adsorption of the carboxylic acids (*n*-butyric acid) on the silica gel is shown. According to a number of reports[16-23], the heat treatment in vacuo reduces the number of OH groups and changes the nature of S–O bonds. The OH groups on the silica gel were not exterminated by the usual calcination, and a greater part of the group are thought to remain in the samples of the present study. The unclosed hysteresis loop of the *n*-butyric acid is presumed to be due to the chemisorption with these residual OH groups. When the adsorption-desorption process is repeated once again from a point $P/P_0=0$, the loop returns back to the original point as is seen in Fig. 9. Clearly the second adsorption process was physical in nature, and no anomality appears in further repetitions of the process.

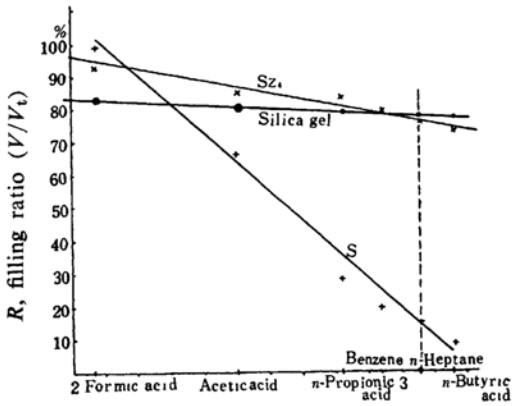

Fig. 10. Sieving coefficient.

16) J. J. Kipling and D. B. Peakall, ibid., 1957, 834.
17) J. H. de Boer, M. E. A. Hermans and J. M. Vleeskens, *Konnikl. Ned. Akad. Wetenschap. Proc., Ser.* **B60**, 45 (1957).
18) J. H. D. de Boer and J. W. Vleeskens. ibid., **B60**, 234 (1957).
19) L. D. Belyakova and A. V. Kiselev, *Doklady Akad. Nauk S. S. S. R.*, **119**, 298 (1958).
20) A. V. Kiselev, V. V. Khopina and Yu. A. Elekov, *Izvest. Akad. Nauk S. S. S. R., Chem. Sci. Sec.*, 664 (1958).
21) K. G. Krasil'nikov, V. F. Kiselev and E. T. Sysoec., *Doklady Akad. Nauk S. S. S. R.*, **116**, 990 (1957).
22) S. P. Zhdanow and A. V. Kiselev., *Zhur. Fiz. Khim.*, **31**, 2213 (1957).
23) D. D. Belvakova, O. M. Dzhigit and A. V. Kiselev, ibid., **31**, 1577 (1958).

In Fig. 10, the filling ratio, $R=V/V_t$, is plotted against the radii of the adsorption sectional area of the adsorbate molecules, r, where V_t is the total volume of adsorbent (Tables IV and VII) and V, the total volume of the adsorbate adsorbed on the adsorbent (Table VII).

TABLE VII. ADSORBED VOLUME, A, OF ADSORBATES AT $P/P_0=1.0$

Adsorbate	Adsorbed volum, V		
	S_4	SZ_4	Silica gel
Formic acid	0.21	1.06	0.41
Acetic acid	0.14	0.97	0.40
n-Propionic acid	0.06	0.95	0.39
Benzene	0.04	0.90	0.387
n-Heptane	0.03	0.86	0.38
n-Butyric acid	0.018	0.83	0.38
Total pore vol., V_t	0.2126	1.142	0.4960

The adsorbed volume was calculated on the assumption that the density of the adsorbed liquid is the same as that in bulk. As for the *n*-heptane, the length and width of the molecule is reported to be 11.6 and 4.9Å, respectively, but the radius of the cross section, r, is unknown. If the values of the filling ratio of *n*-heptane are marked on the lines in Fig. 10, the three points lie on a line which meets with the abscissa at right angles. The radius can be estimated from the cut on the abscissa as 3.05Å which is proper in order of magnitude compared with the width.

The filling ratios change linearly with the radii of the adsorptive sectional area for respective adsorbents. The new term "sieving coefficient" is defined as the slope of these lines, which signifies an ability of the physical selective adsorption or the sieving effect. The sieving coefficient increases with the sharpness of the peak in the pore-size distribution curve. The coefficients for the adsorbents studied are as follows:

S_4 0.947_3, SZ_4 0.155_5, Silica gel No. 28 0.057.

The sieving coefficient would be quite a useful term to specify the adsorptive behavior of the adsorbents.

Summary

1. The adsorption characteristics of the sugar carbon prepared by carbonization or activation and silica gel were studied in detail by the adsorption of water, benzene and fatty acid vapors, and mercury porosimetry.

The pore distribution of the active carbon was tri-disperse. The effects of the partial filling of the pores were examined. The missing link in the distribution curve between the micro-pore and transitional pore in the previous reports was replenished.

2. The narrow-neck or ink-bottle structure of the pores of sugar carbon complicated the adsorption characteristics. The pores of the silica gel were cylindrical with a uniform section.

3. In order to specify the physical selective adsorption, the new term "sieving coefficient" was defined from the relation between the pore radii and cross sections of the adsorbates.

The author expresses his gratitude to Professor I. Sano of Nagoya University for his encouragement.

Department of Chemistry
Nagoya Municipal Industrial
Research Institute
Atsuta-ku, Nagoya